Geophysical Research Letters

RESEARCH LETTER
10.1029/2019GL085086

Orographic Controls on Subdaily Rainfall Statistics and Flood Frequency in the Colorado Front Range, USA

Matthew W. Rossi[1,2], **Robert S. Anderson**[3,4], **Suzanne P. Anderson**[3,4], and **Gregory E. Tucker**[2,3]

[1]Earth Lab, University of Colorado Boulder, Boulder, CO, USA, [2]Cooperative Institute for Research in Environmental Sciences, University of Colorado Boulder, Boulder, CO, USA, [3]Department of Geological Sciences, University of Colorado Boulder, Boulder, CO, USA, [4]Institute of Arctic and Alpine Research, University of Colorado Boulder, Boulder, CO, USA

Key Points:
- Magnitudes of rainfall-triggered runoff events peak at lower mountain elevations in the Colorado Front Range
- Orographic gradients in subdaily rainfall statistics are weak, suggesting other causes of efficient runoff generation at lower elevations
- We hypothesize instead that patterns in critical zone structure (e.g., exposed bedrock, soil depth) enhance runoff at lower elevations

Supporting Information:
- Supporting Information S1

Correspondence to:
M. W. Rossi,
matthew.rossi@colorado.edu

Citation:
Rossi, M. W., Anderson, R. S., Anderson, S. P., & Tucker, G. E. (2020). Orographic controls on subdaily rainfall statistics and flood frequency in the Colorado Front Range, USA. *Geophysical Research Letters*, *47*, e2019GL085086. https://doi.org/10.1029/2019GL085086

Received 20 AUG 2019
Accepted 11 NOV 2019
Accepted article online 15 NOV 2019

Abstract Generalizable relationships for how subdaily rainfall statistics imprint into runoff statistics are lacking. We use the Colorado Front Range, known for destructive rainfall-triggered floods and landslides, to assess whether orographic patterns in runoff generation are a direct consequence of rainstorm climatology. Climatological analysis relies on a dense network of tipping-bucket rain gauges and gridded precipitation frequency estimates from the National Oceanic and Atmospheric Administration to evaluate relationships among subdaily rainfall statistics, topography, and flood frequency throughout the South Platte River basin. We find that event-scale rainfall statistics only weakly depend on elevation, suggesting that orographic gradients in runoff "extremes" are not simply a consequence of rainfall patterns. In contrast, bedrock exposure strongly varies with elevation in a way that plausibly explains enhanced runoff generation at lower elevations via reduced water storage capacity. These findings are suggestive of feedbacks between bedrock river evolution and hillslope hydrology not typically included in models of landscape evolution.

Plain Language Summary Large floods generated along the eastern slopes of the Colorado Front Range, USA, threaten communities near the transition between the Great Plains and Colorado Rockies. While seasonal snowpack and snowmelt control mean water supply and streamflow, runoff generated during rare, intense rainstorms at lower mountain elevations generates the largest floods in this region. In this work, we assess how well spatial patterns in flood frequency mirror rainstorm properties. We find that patterns in subdaily properties of rainstorms (i.e., intensities, durations) fail to explain the differences in the sizes of the largest floods. Instead, we show how "rockiness" strongly decreases with increasing elevation in the unglaciated part of the landscape and hypothesize that systematic differences in land surface properties (such as infiltration capacity and soil depth) may amplify the runoff response to rare rainfall events at low to intermediate mountain elevations. These results highlight the need for better constraints on elevation-dependent properties of the land surface. Such properties may be as important to explaining spatial patterns in the frequency of floods as is understanding the climatology of "extreme" rainfall itself.

1. Introduction

Orographic precipitation is important to water resources, ecosystem dynamics, natural hazards, and the long-term evolution of mountain ranges (Roe, 2005). However, characterizing orographic patterns in precipitation in mountain landscapes is challenging due to sparse observations. For example, space-borne remote sensing has only recently revealed how landscape-scale patterns in topographic relief can concentrate mean rainfall in narrow bands (e.g., the Himalayas; Anders et al., 2006; Bookhagen & Burbank, 2006) that are spatially distinct from "extreme" rainfall climatology (Deal et al., 2017). Yet such remote sensing data are relatively coarse (~5 to 30-km pixels for Tropical Rainfall Measuring Mission data) and thus limited in resolving small-scale, high-intensity convective storms that prevail in some settings. Even less is known about how orographic patterns in rainfall and runoff will respond to modern climate change, although intensities of short-duration rainstorms are likely changing the most (e.g., Westra et al., 2014). Climate change studies focusing on modeled and observed increases in precipitation frequencies often carry an implicit assertion that precipitation changes (whether in phase or rates) are the key unknown to flooding. However, direct relationships between precipitation and runoff statistics are not borne out by the historic record, likely due to antecedent

moisture dynamics, land-cover patterns, snow hydrology, and scaling properties of rainstorms (e.g., Sharma et al., 2018). These challenges together motivate the need for better use of dense observational networks in mountain landscapes, where they exist. While many studies analyze rain gauge data, only a few use subdaily rainfall to characterize orographic controls on event statistics (Allamano et al., 2009; Avanzi et al., 2015). We address this knowledge gap by characterizing orographic controls on subdaily rainfall statistics in the Colorado Front Range (CFR), USA, and directly contrast these patterns against those in flood frequencies.

The eastern slopes of the CFR are known for generating destructive events like the 1976 Big Thompson flood (Costa, 1978), the 1997 Fort Collins flood (Ogden et al., 2000), and the 2013 CFR floods (Moody, 2016) and landslides (Anderson et al., 2015; Coe et al., 2014). Given the high hazard, the specific meteorological conditions that led to these events (Maddox et al., 1980; Petersen et al., 1999; and Gochis et al., 2015, respectively) are known. Paleohydrological studies set the context for these historic events and show that such large floods typically arise at low to intermediate elevations in the CFR (England et al., 2010; Jarrett, 1990), even though mean annual precipitation is highest at the crest of the watersheds. Based on this, Jarrett (1990) proposed that the climatology of flooding changes abruptly at outlet elevations of ~2,300 m, whereby rainfall triggers peak flows at lower elevations and snowmelt triggers peak flows at higher elevations. Subsequent analyses support this claim by showing that snowmelt causes relatively smaller peak annual floods (Fassnacht & Records, 2015; Pitlick, 1994) and that this is attributable to the fraction of time snow covers the surface, which itself depends on watershed hypsometry (Kampf & Lefsky, 2016). Implicit to such interpretations is that peak snowmelt runoff is smaller relative to rainfall runoff because some property of rainfall events (e.g., intensity, duration, depth) is enhanced at low to intermediate elevations. However, daily precipitation data in the CFR suggest that intense precipitation occurs at all elevations and at any time of year, seemingly at odds with strong orographic gradients in rainfall-triggered runoff (Mahoney et al., 2015).

A major target of this work is to evaluate how much hydrologic realism is needed to characterize orographic patterns in flood frequency in steep, eroding landscapes, with an eye toward improving landscape evolution models that incorporate stochastic rainfall (e.g., Deal et al., 2018; Tucker, 2004). Such models necessarily simplify hydrology because they represent erosional dynamics over long time scales. Our first objective is therefore to evaluate whether orographic patterns in subdaily rainfall statistics explain differences in flood frequency observed at river gauges throughout the South Platte River Basin. We find that spatial patterns in subdaily rainfall statistics are weak. In contrast, topographic proxies for bedrock exposure show large relative differences as a function of elevation. Based on this, we hypothesize that systematic patterns in land surface properties that affect water storage capacity enhance rainfall runoff at lower mountain elevations.

2. Data and Methods

We assemble data primarily from six sources: (1) United States Geological Survey (USGS) daily streamflow data (https://maps.waterdata.usgs.gov/mapper/); (2) Atlas-14 precipitation frequency estimates from National Oceanic and Atmospheric Administration (NOAA) (https://hdsc.nws.noaa.gov/pub/hdsc/data/mw/); (3) subdaily rainfall data from the Urban Drainage and Flood Control District (http://alert5.udfcd.org/); (4) USGS 1 arc-second topography (https://viewer.nationalmap.gov/basic/); (5) 2010 lidar topography for the Boulder Creek watershed (https://opentopography.org/); and (6) 2018 aerial imagery from Pictometry® (https://www.arcgis.com/). Two other data sources are also used in the Supporting Information: the Parameter-elevation Relationships on Independent Slopes Model (PRISM) (http://www.prism.oregonstate.edu/), and the Global Historical Climate Network daily data (https://www.ncdc.noaa.gov/ghcn-daily-description).

Watershed-scale runoff analysis relies on data from gauges in the South Platte River basin (Figure 1). Following Kampf and Lefsky (2016), we select watersheds in which flow modification least impacts high flows. All but two gauges from this prior analysis are used but with data available through 2017. We also include four gages that Kampf and Lefsky (2016) rejected because of inactivity, but that represent large tributaries of the South Platte River with long records. For each gauged watershed, we calculated average elevation and the shape of the right tail of probability distributions of daily runoff (daily streamflow divided by drainage area). This latter task uses rank frequency to calculate exceedance probabilities and the stretched exponential distribution to fit events above those that occur, on average, five times per year (e.g., Rossi

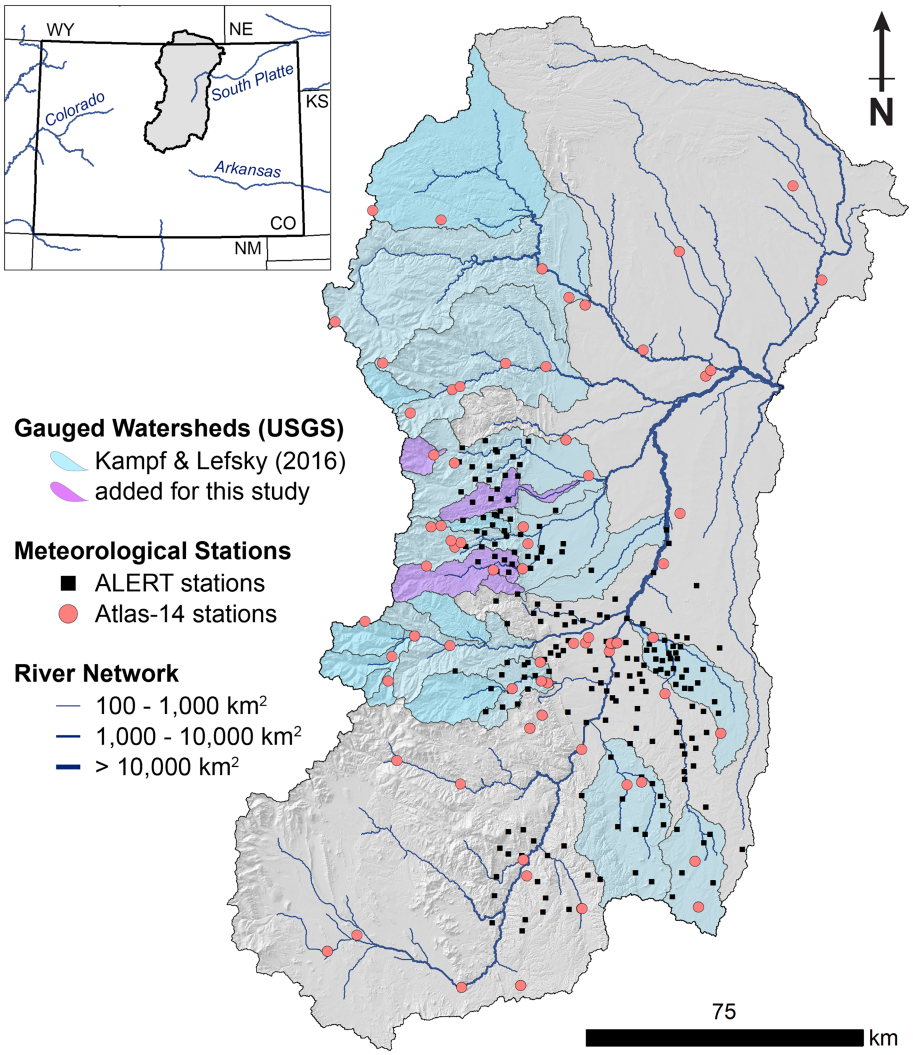

Figure 1. (Main) The upper South Platte River study area (inset) drains north central Colorado and small portions of south central Wyoming. The main panel shows locations of meteorological stations and gauged watersheds used. Darker shading indicates catchment nesting.

et al., 2016). Small values of the shape parameter, *c*, in the stretched exponential distribution indicate high variability runoff, whereas large values indicate low variability. Detailed explanation of watershed selection, delineation, and analysis is in Supporting Information Figure S1, Table S1, and Texts S1 and S3.

Event-scale rainfall analysis relies on two data products. First, we use precipitation frequencies with 90% confidence levels from Atlas-14 vol. 8 v. 2.0 (Perica et al., 2013). This gridded product largely uses time series data from COOP and SNOTEL meteorological stations of variable record length (Figure 1) with spatial interpolation algorithms that build on PRISM data (Daly et al., 2008). Atlas-14 precipitation frequencies span 5-min to 60-day intervals and recurrence times of 1 to 1,000 years. Second, we use the ALERT network, an early warning system for flash floods in the Denver metropolitan area, as an independent network of 200 tipping-bucket rain gauges that generates high spatial density observations of subdaily rainfall rates. Gauges are unheated and do not reliably record snowfall. Each bucket tip records the accumulation time for 1 mm of rainfall. ALERT allows us to evaluate event-scale rainfall statistics (intensity, duration, depth) along the transition from the Great Plains up into higher elevations of the CFR. We adopt a practical set of rainfall measurement thresholds (which vary by averaging interval) to identify events such that short, intense convective storms common to the CFR can be resolved. Detailed explanation of ALERT data, event identification, the influence of snowfall, and time series analysis is in Supporting Information Figures S2–S7, Tables S2 and S3, and Texts S2 and S3.

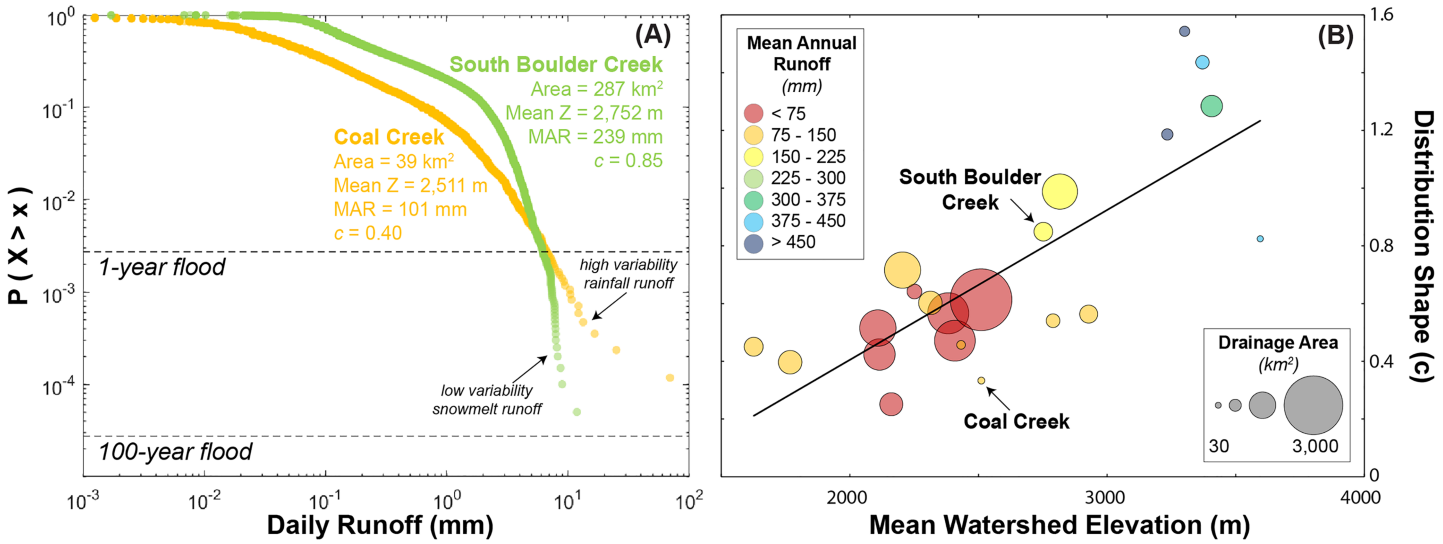

Figure 2. (A) Exceedance probability, $P(X > x)$, of runoff for neighboring stream gauges and (B) the relationship between mean watershed elevation and the best fit shape parameter, c, for all gauges shown in Figure 1. In A, Coal Creek data span 1959–1982 and South Boulder Creek data span 1896–1995 (only data before 1954 are shown to avoid impact of Gross Dam). In B, fits do not account for water diversions and dams. However, careful site selection minimizes the impact of water management on extreme event frequencies.

Bedrock exposure analysis is based on a 1-m digital elevation model derived from airborne lidar acquired by the National Center for Airborne Laser Mapping for the Boulder Creek Critical Zone Observatory (Anderson et al., 2012). We follow DiBiase et al. (2012) and use a slope threshold to distinguish bedrock from colluvium. Slope thresholds are calibrated against Pictometry® imagery for eight patches that span different geomorphic process domains over a large range of elevations. Using the calibrated proxy, we calculated the fraction of bedrock within 25-m elevation bins throughout the Boulder Creek watershed. Detailed explanation of lidar data, topographic proxies for bedrock, and elevation-dependent relationships for bedrock is in Supporting Information Figures S8–S12, Table S4, and Text S4.

3. Runoff Analysis

Results of daily runoff analysis are summarized in Figure 2. Figure 2A is an exceedance probability plot for two neighboring watersheds, one of which drains low to intermediate elevations (Coal Creek) while the other drains up to the Continental Divide (South Boulder Creek). These exemplar stations illustrate how the shape of the right tail of runoff distributions differs among watersheds in the CFR. In general, higher elevation watersheds exhibit less variability in runoff (i.e., higher values of the shape parameter, c) (Figure 2B). This reflects increased snow persistence at higher elevations (Kampf & Lefsky, 2016) and is consistent with a snowmelt signature on flood frequency distributions observed in regional (Pitlick et al., 1994; Fassnacht & Records, 2015) and national (Berghuijs et al., 2016; Rossi et al., 2016) analyses. The shape parameter of the runoff distribution encodes the ratio of magnitudes of rare to intermediate frequency events. As such, high-variability distributions can arise from either smaller, intermediate frequency events or larger, rare ones. The distinction is important, because the former is due to less efficient runoff generation during moderate frequency events, while the latter suggests more efficient runoff generation during rare events. The exemplar stations in Figure 2A show more efficient runoff generation in the lower-elevation watershed for events larger than ~1-year flow. However, this explanation is not ubiquitous among subcatchments within the South Platte River basin. For example, lower-elevation watersheds that primarily drain High Plains terrain show higher runoff variability than their alpine to subalpine counterparts (Figure 2B) yet also exhibit lower peak daily values over the historic record (Figure S1). Taken together, these findings support the notions that elevation-dependent relationships for flood frequency in the CFR are due to the transition from snowmelt- to rainfall-triggered extremes (Jarrett & Costa, 1988; Kampf & Lefsky, 2016) and that peak runoff generation optimizes at lower mountain elevations, echoing Jarrett (1990) (see his Figure 4). There are three possible explanations for a mid-elevation optimum: (1) rare storms at mid-elevations generate

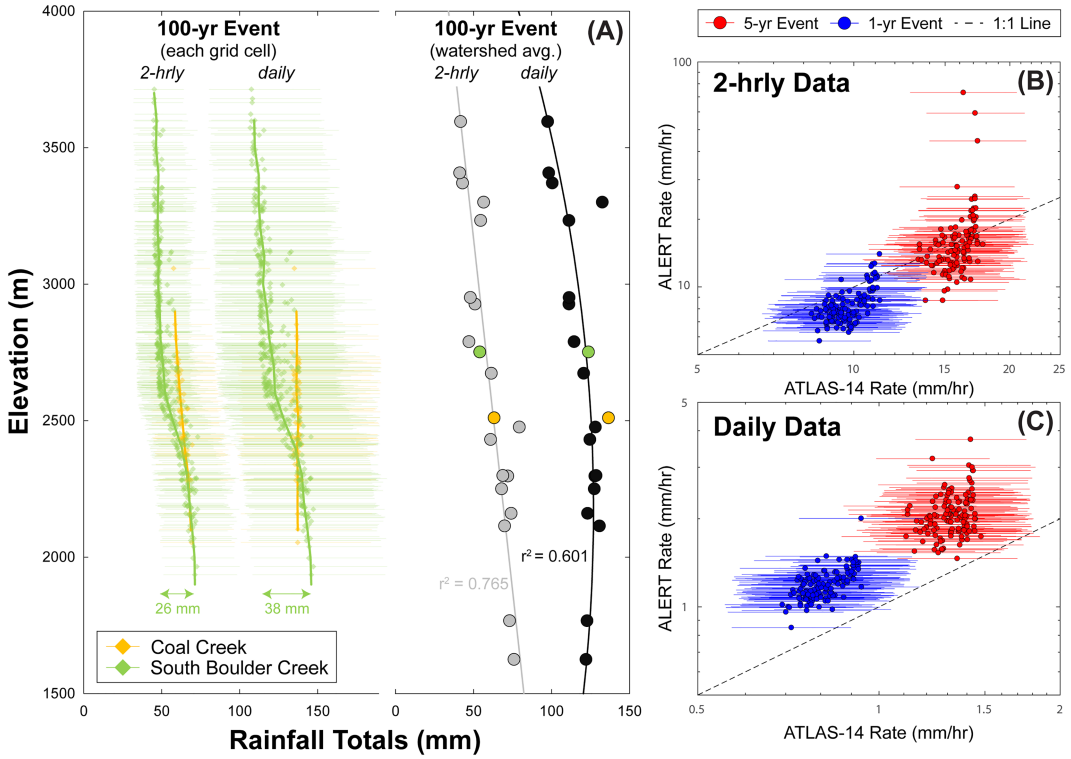

Figure 3. (A) Relationship between elevation and 100-year rainfall events from Atlas-14, and comparisons of Atlas-14 against ALERT rain rates for (B) 2-hourly and (C) daily data. In A, the left panel shows grid cell values and 90% confidence limits for the watersheds in Figure 2A. Bold lines are elevation-binned averages for these data (100-m bins). The right panel shows similar relationships for watershed-averaged values of 100-year rainfall rates (sans two watersheds partially in Wyoming).

more runoff due to higher intensities and durations; (2) rare storms at high elevations produce more solid-phase precipitation that must melt before runoff occurs, inhibiting flashy runoff; or (3) elevation-dependent properties of the surface make mid-elevations more conducive to runoff generation. We explicitly assess the former in section 4 and the latter in section 5, with a full discussion of all three explanations in section 6.

4. Rainfall Analysis

To examine whether "extreme" runoff climatology is directly attributable to rainstorm properties, we first ask whether rainfall event statistics are concordant with orographic gradients in runoff statistics. We then ask whether rainstorm statistics account for differences in the magnitudes of rare floods. Figure 3A shows parametric estimates of 100-year precipitation rates from Atlas-14. While Atlas-14 is widely used for hazard assessment, its limitations are well known, especially under nonstationary climate (e.g., Wright et al., 2019). For this study, the two key caveats in using Atlas-14 frequency estimates are that estimates are interpreted as representing rainfall events for long recurrence times even though snow is included in frequency estimation and that spatial interpolation is built on PRISM-derived mean annual maxima, which is itself elevation-dependent (Perica et al., 2013). The left side of Figure 3A shows 2-hourly and 24-hourly rainfall totals for each grid cell in the South Boulder and Coal Creek watersheds (compare to Figure 2A). We consider the end-member scenario in which all parts of the watersheds receive their 100-year rainfall rates synchronously. To the degree that rare events are not spatially correlated (e.g., due to small convective storms), the inferred watershed-averaged value will be less than this end-member case. While orographic gradients in the 100-year, daily rainfall totals within a watershed span up to 38 mm (Figure 3A, left), the watershed-averaged difference between 100-year events for South Boulder and Coal Creek is ~13 mm. These two watersheds are representative of other subcatchments in the basin (Figure 3A, right). Atlas-14 shows a roughly

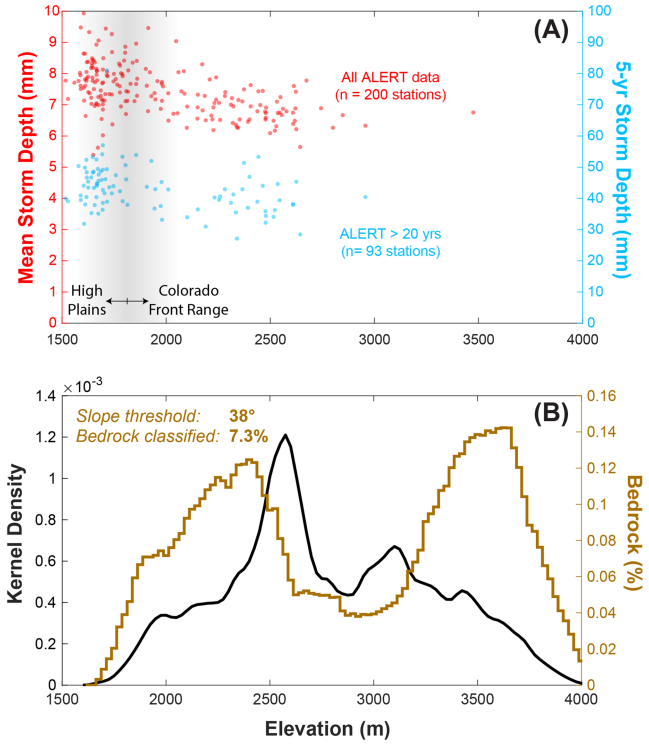

Figure 4. Relationships with elevation for (A) ALERT-derived storm depths and (B) lidar-derived areal fraction (left axis) and bedrock fraction (right axis). In A, storm depths are calculated from 1-hourly data. Events begin when rainfall rates exceed 2 mm/hr and end when rates drop below threshold for 2 hr. Shading shows approximate boundary between High Plains and CFR. In B, kernel density estimates of elevation for the Boulder Creek watershed use a 25-m bandwidth and normal smoothing function. Bin sums of bedrock use 25-m elevation bins.

linear decrease in 2-hourly rainfall rates with watershed-averaged elevation and a nonlinear relationship for daily rainfall rates, with maximum values at ~2,500 m and below.

We also compare Atlas-14 frequencies against empirical estimates from ALERT stations that have at least 20 years of record (Figures 3B and 3C). This guarantees that at least four observed events constrain higher recurrence times (i.e., 5-year events). Daily rainfall rates derived from ALERT data are substantially higher than those from Atlas-14 at both the 1- and 5-year recurrence times (Figure 3C). This is somewhat surprising given that most stations used to construct Atlas-14 record daily observations. We offer three interpretations: (1) ALERT stations are biased toward the present, which may be an interval with more intense storms than the longer-term averages used in Atlas-14; (2) inclusion of snowfall in Atlas-14 underpredicts rainfall rates with moderate recurrence times; and (3) Atlas-14 precipitation frequency estimates underpredict daily rainfall rates in the CFR. Empirical estimates of 2-hourly rainfall rates from ALERT stations largely overlap Atlas-14 predictions within uncertainty (Figure 3B). While it is unclear why Atlas-14 would perform better over shorter time intervals, Figure 3b does suggest that temporal interpolation in Atlas-14 reasonably approximates rainfall rates during such events. However, the slope of the relationship shown in Figure 3B is steeper than unity, meaning that a number of ALERT stations show much higher intensities than predicted by Atlas-14. While suggestive of more variable rainfall rates than predicted by Atlas-14, the subdaily time series data are too short to evaluate this claim quantitatively.

Using ALERT data alone, we also evaluate whether orographic trends in subdaily rainfall statistics emerge directly from observations. ALERT stations are unaffected by interpolation choices and are minimally impacted by the confounding variable of snowfall (see Figure S5 and Table S3). While process (e.g., landslides, floods) will dictate which rainstorm metrics are most relevant (e.g., intensity, duration, depth), Figure 4A summarizes our findings for storm depth because it shows the "clearest" orographic trend. If rainfall rates and durations are cross-correlated, storm depth may better reveal orographic gradients in rainfall fluxes than looking at rainfall rates alone (e.g., Figure 3) (see Figure S6 for other metrics). Correlations between either mean storm depths or 5-year storm depths with elevation are weak (Figure 4A) but do reveal a modest decrease in these values that is consistent with decreases in event-scale runoff variability (Figure 2B). However, because variations in the mean and the 5-year storm depths between stations are much larger than the trends, caution is warranted in relating storm depth statistics to patterns in flood frequency.

5. Bedrock Exposure Analysis

To assess the plausibility that systematic variations in land surface properties are responsible for patterns of runoff generation in the CFR, we use a calibrated slope-threshold proxy of 38° (see Figures S8–S11) on 1-m topography for the Boulder Creek watershed to quantify bedrock exposure as a function of elevation (following DiBiase et al., 2012; Marshall & Roering, 2014). While the presence of tors, or emergent outcrops within a soil-mantled surface, causes the simple slope threshold to underestimate bedrock by up to 10%, relative patterns in bedrock exposure are robust as long as sufficiently high thresholds are used (see Figures S11 and S12 and Table S4). Figure 4B shows fractional area and fractional bedrock in the Boulder Creek watershed as functions of elevation. Two bedrock modes emerge: (1) a higher elevation mode due to bedrock cliffs in the glaciated part of the landscape, and (2) a lower-elevation mode associated with more rugged topography and higher erosion rates observed at and below fluvial knickzones. This lower mode suggests a threefold

contrast in exposed bedrock in the fluvially dominated part of the landscape below the zone of Pleistocene glaciation (Figure 4B). These findings are consistent with lower water storage capacity and thus higher efficiency of runoff generation at low to intermediate elevations.

6. Discussion

Our subdaily rainfall analysis supports regional analyses showing weak trends in daily precipitation with elevation (Mahoney et al., 2015). Although "extreme" precipitation events at higher elevations sometimes occur as hailstorms less likely to cause flash flooding (Cotton et al., 2003), simulations resolving hailstorms show that such events account for <20% of events even near the Continental Divide (Mahoney et al., 2012). Consequently, Mahoney et al. (2015) argued against previously proposed elevation limits (at ~2,500 m) to rainfall-triggered flooding in the CFR (Cotton et al., 2003; Jarrett, 1993). We reexamined this question using direct observations of subdaily rainfall rates (ALERT) that minimize the influence of solid-phase events. While ALERT only contains a handful of stations above 2,500 m, these stations show evidence of frequent, intense rainfall events that are only marginally smaller than those observed at lower elevations (Figures 4A, S6, and S7). However, weak orographic gradients in rainfall statistics need not call into question proposed elevation limits to flash flooding in the CFR. Maxima in runoff generation at lower mountain elevations during peak flows in the CFR (e.g., Jarrett, 1990; Kampf & Lefsky, 2016) are also observed in the daily runoff distributions presented here (Figures 2A and S1). Extrapolation of exceedance probabilities in Figure 2A suggest that the difference in 100-year runoff events between two exemplar watersheds is >80 mm/day. This is sixfold larger than the associated ~13 mm/day enhancement of rainfall rates shown in Figure 3A. We therefore propose that some other elevation-dependent property of the CFR amplifies the conversion of rainfall to runoff at lower mountain elevations.

Hydrologic models that use stochastic rainfall to generate runoff place high importance on the interaction between storm depth distributions and the effective storage capacity of the watershed (e.g., Doulatyari et al., 2015). Watershed storage influences sensitivity to the rainfall forcing because of nonlinearities in the hydrological system (e.g., Vivoni et al., 2007) that arise from hillslope runoff generation dynamics and scaling properties of the watershed (Sivapalan et al., 2002). Heterogeneous soil depths and textures, dynamic soil moisture and plant water use, and surface water transit, including the buffering capacity of lakes and floodplains, each impact watershed-scale storage. In the CFR, we show that bedrock exposure, and thus the fraction of impervious area, is higher at lower mountain elevations. Bedrock exposure is one of several properties that may reduce watershed-scale storage with elevation as relief is generated in a mountain range. Increased bedrock exposure is linked to thinner soils (e.g., Heimsath et al., 2012) which, in turn, lowers water storage capacity and shortens water transit times (e.g., Clow et al., 2018). The glaciated, alpine topography reflected in the high elevation mode of increased bedrock exposure (Figure 4B) is characterized by broad valleys and moraine-dammed lakes that enhance surface water storage during rainstorms, perhaps explaining why flashy runoff is not observed in this otherwise "rocky" terrain. We do not quantify each of these effects but instead propose that their collective contribution to event-scale water storage helps reconcile the lack of strong orographic controls on subdaily rainfall statistics and the seemingly contradictory claims of Mahoney et al. (2015) and Jarrett (1993).

Our findings also pose an intriguing suite of possible feedbacks among fluvial incision, hillslope hydraulic properties, and stochastic rainfall. Fluvial knickpoints in the CFR (Anderson et al., 2006) divide the landscape into slowly eroding upstream catchments (~25 m/Ma) and more rapidly eroding settings at and below knickzones (~150 m/Ma along mainstem; ~30–60 m/Ma along downstream tributaries) (Dethier et al., 2014). As erosion exceeds soil production, more bedrock is exposed, soils thin, and colluvial cover becomes patchy (Heimsath et al., 2012). In the CFR, bedrock is relatively abundant, suggesting that erosion rates are near limits to soil production. "Rockiness" is concentrated at lower mountain elevations, consistent with the upstream migration of erosional signals in response to an increase in base level fall (e.g., Anderson et al., 2006; Rosenbloom & Anderson, 1994; Whipple & Tucker, 1999). Such signals may produce spatially explicit feedbacks among the evolving river network, critical zone structure, and watershed-scale storage for any landscape responding to a change in climate or tectonics. Whereas conventional treatments of orographic effects on river incision focus on the phase and fluxes of precipitation inputs (e.g., Anders et al., 2008), we argue for commensurate efforts to quantify variations in land

surface properties with elevation and local relief. Such data could serve as the basis for testing feedbacks among hydroclimatic forcing, topography, and land surface properties in more fully coupled models of hydrology and landscape evolution.

7. Conclusions

Analysis of daily streamflow data corroborates prior flood frequency and paleohydrologic studies using annual maxima to show that large floods are generated by rainfall events at lower mountain elevations in the CFR, USA. For 2-hourly rates, gridded precipitation frequency estimates from NOAA reasonably match empirical exceedance frequencies derived from an independent network of tipping-bucket rain gauges. At 24-hourly intervals, NOAA rates are systematically lower than implied by gauge data. Both data products suggest a weak orographic gradient in subdaily rainfall statistics that is insufficient to explain the generation of the largest runoff events at lower mountain elevations. In contrast, we show that bedrock exposure is much higher at lower mountain elevations and hypothesize that it is the spatial variation in land surface properties such as bedrock exposure, soil hydraulics, and surface water connectivity that enhance runoff generation. Critical zone structure is the filter through which rainfall must pass, potentially governing orographic patterns in the generation of the region's largest floods.

Acknowledgments
Source code and data are available online (at https://github.com/mwrossi/cfr_extremes). Support for this research came from the Geomorphology and Land-use Dynamics Program at the National Science Foundation (EAR-1822062), the Boulder Creek Critical Zone Observatory (EAR-1331828), and Earth Lab, a synthesis center developed under the University of Colorado at Boulder's Grand Challenge Initiative. We thank the AE, one anonymous reviewer, and S. Kampf for constructive comments that improved the quality of this manuscript.

References

Allamano, P., Claps, P., Laio, F., & Thea, C. (2009). A data-based assessment of the dependence of short-duration precipitation on elevation. *Physics and Chemistry of the Earth*, *34*(10-12), 635–641. https://doi.org/10.1016/j.pce.2009.01.001

Anders, A. M., Roe, G. H., Hallet, B., Montgomery, D. R., Finnegan, N. J., & Putkonen, J. (2006). Spatial patterns of precipitation and topography in the Himalaya. *Geological Society of America Special Papers*, *398*, 39–53. https://doi.org/10.1130/2006.2398(03)

Anders, A. M., Roe, G. H., Montgomery, D. R., & Hallet, B. (2008). Influence of precipitation phase on the form of mountain ranges. *Geology*, *36*(6), 479–482. https://doi.org/10.1130/G24821A.1

Anderson, R., Riihimaki, C., Safran, E., & MacGregor, K. (2006). Facing reality: Late Cenozoic evolution of smooth peaks, glacially ornamented valleys, and deep river gorges of Colorado's Front Range. *Geological Society of America Special Papers*, *398*, 397–418. https://doi.org/10.1130/2006.2398(25)

Anderson, S. P., Qinghua, G., & Parrish, E. G. (2012). Snow-on and snow-off Lidar point cloud data and digital elevation models for study of topography, snow, ecosystems and environmental change at Boulder Creek Critical Zone Observatory, Colorado: Boulder Creek CZO, INSTAAR, University of Colorado at Boulder. *Digital Media*. https://doi.org/10.5069/G93R0QR0

Anderson, S. W., Anderson, S. P., & Anderson, R. S. (2015). Exhumation by debris flows in the 2013 Colorado Front Range storm. *Geology*, *43*(5), 391–394. https://doi.org/10.1130/G36507.1

Avanzi, F., De Michele, C., Gabriele, S., Ghezzi, A., & Rosso, R. (2015). Orographic signature on extreme precipitation of short durations. *Journal of Hydrometeorology*, *16*(1), 278–294. https://doi.org/10.1175/JHM-D-14-0063.1

Berghuijs, W. R., Woods, R. A., Hutton, C. J., & Sivapalan, M. (2016). Dominant flood generating mechanisms across the United States. *Geophysical Research Letters*, *43*, 4382–4390. https://doi.org/10.1002/2016GL068070

Bookhagen, B., & Burbank, D. W. (2006). Topography, relief, and TRMM-derived rainfall variations along the Himalaya. *Geophysical Research Letters*, *33*,LO8405. https://doi.org/10.1029/2006GL026037

Clow, D. W., Mast, M. A., & Sickman, J. O. (2018). Linking transit times to catchment sensitivity to atmospheric deposition of acidity and nitrogen in mountains of the western United States. *Hydrological Processes*, *32*(16), 2456–2470.

Coe, J. A., Kean, J. W., Godt, J. W., Baum, R. L., Jones, E. S., Gochis, D. J., & Anderson, G. S. (2014). New insights into debris-flow hazards from an extraordinary event in the Colorado Front Range. *GSA Today*, *24*(10), 4–10. https://doi.org/10.1130/GSATG214A.1

Costa, J. E. (1978). Colorado Big Thompson flood: Geologic evidence of a rare hydrologic event. *Geology*, *6*(10), 617–620. https://doi.org/10.1130/0091-7613(1978)6<617:CBTFGE>2.0.CO;2

Cotton, W. R., McAnelly, R. L., & Ashby, T. (2003). *Development of new methodologies for determining extreme rainfall*. Dept. of Natural Resources, State of Colorado. 140 p.

Daly, C., Halbleib, M., Smith, J. I., Gibson, W. P., Doggett, M. K., Taylor, G. H., et al. (2008). Physiographically sensitive mapping of climatological temperature and precipitation across the conterminous United States. *International Journal of Climatology*, *28*(15), 2031–2064. https://doi.org/10.1002/joc.1688

Deal, E., Braun, J., & Botter, G. (2018). Understanding the role of rainfall and hydrology in determining fluvial erosion efficiency. *Journal of Geophysical Research, F: Earth Surface*, *123*(4), 744–778. https://doi.org/10.1002/2017JF004393

Deal, E., Favre, A. C., & Braun, J. (2017). Rainfall variability in the Himalayan orogen and its relevance to erosion processes. *Water Resources Research*, *53*, 4004–4021. https://doi.org/10.1002/2016WR020030

Dethier, D. P., Ouimet, W., Bierman, P. R., Rood, D. H., & Balco, G. (2014). Basins and bedrock: Spatial variation in 10Be erosion rates and increasing relief in the southern Rocky Mountains, USA. *Geology*, *42*(2), 167–170. https://doi.org/10.1130/G34922.1

DiBiase, R. A., Heimsath, A. M., & Whipple, K. X. (2012). Hillslope response to tectonic forcing in threshold landscapes. *Earth Surface Processes and Landforms*, *37*(8), 855–865. https://doi.org/10.1002/esp.3205

Doulatyari, B., Betterle, A., Basso, S., Biswal, B., Schirmer, M., & Botter, G. (2015). Predicting streamflow distributions and flow duration curves from landscape and climate. *Advances in Water Resources*, *83*, 285–298. https://doi.org/10.1016/j.advwatres.2015.06.013

England, J. F., Godaire, J. E., Klinger, R. E., Bauer, T. R., & Julien, P. Y. (2010). Paleohydrologic bounds and extreme flood frequency of the Upper Arkansas River, Colorado, USA. *Geomorphology*, *124*(1–2), 1–16. https://doi.org/10.1016/j.geomorph.2010.07.021

Fassnacht, S. R., & Records, R. M. (2015). Large snowmelt versus rainfall events in the mountains. *Journal of Geophysical Research: Atmospheres*, *120*, 2375–2381. https://doi.org/10.1002/2014JD022753

Gochis, D., Schumacher, R., Friedrich, K., Doesken, N., Kelsch, M., Sun, J., et al. (2015). The great Colorado flood of September 2013. *Bulletin of the American Meteorological Society*, *96*(9), 1461–1487. https://doi.org/10.1175/BAMS-D-13-00241.1

Heimsath, A. M., DiBiase, R. A., & Whipple, K. X. (2012). Soil production limits and the transition to bedrock-dominated landscapes. *Nature Geoscience*, *5*(3), 210–214. https://doi.org/10.1038/ngeo1380

Jarrett, R. D. (1990). Paleohydrologic techniques used to define the spatial occurrence of floods. *Geomorphology*, *3*(2), 181–195. https://doi.org/10.1016/0169-555X(90)90044-Q

Jarrett, R. D. (1993). Flood elevation limits in the Rocky Mountains. *Proceedings of the Symposium on Engineering Hydrology*, *180-185*.

Jarrett, R. D., & Costa, J. E. (1988). *Evaluation of the flood hydrology in the Colorado Front Range using precipitation, streamflow, and paleoflood data for the Big Thompson River Basin*. Dept. of Interior, USGS. 87-4117, 37 p.

Kampf, S. K., & Lefsky, M. A. (2016). Transition of dominant peak flow source from snowmelt to rainfall along the Colorado Front Range: Historical patterns, trends, and lessons from the 2013 Colorado Front Range floods. *Water Resources Research*, *52*, 407–422. https://doi.org/10.1002/2015WR017784

Maddox, R. A., Canova, F., & Hoxit, L. R. (1980). Meteorological characteristics of flash flood events over the western United States. *Monthly Weather Review*, *108*(11), 1866–1877. https://doi.org/10.1175/1520-0493(1980)108<1866:MCOFFE>2.0.CO;2

Mahoney, K., Alexander, M. A., Thompson, G., Barsugli, J. J., & Scott, J. D. (2012). Changes in hail and flood risk in high-resolution simulations over Colorado's mountains. *Nature Climate Change*, *2*(2), 125. https://doi.org/10.1038/nclimate1344

Mahoney, K., Ralph, F. M., Wolter, K., Doesken, N., Dettinger, M., Gottas, D., et al. (2015). Climatology of extreme daily precipitation in Colorado and its diverse spatial and seasonal variability. *Journal of Hydrometeorology*, *16*, 781–792. https://doi.org/10.1175/JHM-D-14-0112.1

Marshall, J. A., & Roering, J. J. (2014). Diagenetic variation in the Oregon Coast Range: Implications for rock strength, soil production, hillslope form, and landscape evolution. *Journal of Geophysical Research: Earth Surface*, *119*, 1395–1417. https://doi.org/10.1002/2013JF003004

Moody, J. A. (2016). *Estimates of peak flood discharge for 21 sites in the Front Range in Colorado in response to extreme rainfall in September 2013*. Dept. of Interior, USGS. 2016-5003, 65 p.

Ogden, F. L., Sharif, H. O., Senarath, S. U. S., Smith, J. A., Baeck, M. L., & Richardson, J. R. (2000). Hydrologic analysis of the Fort Collins, Colorado, flash flood of 1997. *Journal of Hydrology*, *228*(1-2), 82–100. https://doi.org/10.1016/S0022-1694(00)00146-3

Perica, S., Martin, D., Pavlovic, S., Roy, I., Laurent, M. S., Trypaluk, C., et al. (2013). *Precipitation-frequency atlas of the United States vol. 8 v. 2*. Dept. of Commerce, NOAA, NWS. 41 p.

Petersen, W. A., Carey, L. D., Rutledge, S. A., Knievel, J. C., Doesken, N. J., Johnson, R. H., et al. (1999). Mesoscale and radar observations of the Fort Collins flash flood of 28 July 1997. *Bulletin of the American Meteorological Society*, *80*(2), 191–216. https://doi.org/10.1175/1520-0477(1999)080<0191:MAROOT>2.0.CO;2

Pitlick, J. (1994). Relation between peak flows, precipitation, and physiography for five mountainous regions in the western USA. *Journal of Hydrology*, *158*(3-4), 219–240. https://doi.org/10.1016/0022-1694(94)90055-8

Roe, G. H. (2005). Orographic precipitation. *Annual Review of Earth and Planetary Sciences*, *33*, 645–671. https://doi.org/10.1146/annurev.earth.33.092203.122541

Rosenbloom, N. A., & Anderson, R. S. (1994). Hillslope and channel evolution in a marine terraced landscape, Santa Cruz, California. *Journal of Geophysical Research - Solid Earth*, *99*(B7), 14,013–14,029. https://doi.org/10.1029/94JB00048

Rossi, M. W., Whipple, K. X., & Vivoni, E. R. (2016). Precipitation and evapotranspiration controls on daily runoff variability in the contiguous United States and Puerto Rico. *Journal of Geophysical Research, F: Earth Surface*, *121*(1), 128–145. https://doi.org/10.1002/2015JF003446

Sharma, A., Wasko, C., & Lettenmaier, D. P. (2018). If precipitation extremes are increasing, why aren't floods? *Water Resources Research*, *54*(11), 8545–8551. https://doi.org/10.1029/2018WR023749

Sivapalan, M., Jothityangkoon, C., & Menabde, M. (2002). Linearity and nonlinearity of basin response as a function of scale: Discussion of alternative definitions. *Water Resources Research*, *38*,(2),1012. https://doi.org/10.1029/2001WR000482

Tucker, G. E. (2004). Drainage basin sensitivity to tectonic and climatic forcing: Implications of a stochastic model for the role of entrainment and erosion thresholds. *Earth Surface Processes and Landforms*, *29*(2), 185–205. https://doi.org/10.1002/esp.1020

Vivoni, E. R., Entekhabi, D., Bras, R. L., & Ivanov, V. Y. (2007). Controls on runoff generation and scale-dependence in a distributed hydrologic model. *Hydrology and Earth System Sciences*, *4*(3), 983–1029. https://doi.org/10.5194/hess-11-1683-2007

Westra, S., Fowler, H. J., Evans, J. P., Alexander, L. V., Berg, P., Johnson, F., et al. (2014). Future changes to the intensity and frequency of short-duration extreme rainfall. *Reviews of Geophysics*, *52*, 522–555. https://doi.org/10.1002/2014RG000464

Whipple, K. X., & Tucker, G. E. (1999). Dynamics of the stream-power river incision model: Implications for height limits of mountain ranges, landscape response timescales, and research needs. *Journal of Geophysical Research - Solid Earth*, *104*(B8), 17,661–17,674. https://doi.org/10.1029/1999JB900120

Wright, D. B., Bosma, C. D., & Lopez-Cantu, T. (2019). US hydrologic design standards insufficient due to large increases in frequency of rainfall extremes. *Geophysical Research Letters*, *46*(14), 8144–8153. https://doi.org/10.1029/2019GL083235

References From Supporting Information

Anderson, R. S. (2002). Modeling the tor-dotted crests, bedrock edges, and parabolic profiles of high alpine surfaces of the Wind River Range, Wyoming. *Geomorphology*, *46*(1-2), 35–58. https://doi.org/10.1016/S0169-555X(02)00053-3

Goodfellow, B. W., Skelton, A., Martel, S. J., Stroeven, A. P., Jansson, K. N., & Hättestrand, C. (2014). Controls of tor formation, Cairngorm Mountains, Scotland. *Journal of Geophysical Research: Earth Surface*, *119*, 225–246. https://doi.org/10.1002/2013JF002862

Habib, E., Krajewski, W. F., & Ciach, G. J. (2001). Estimation of rainfall interstation correlation. *Journal of Hydrometeorology*, *2*(6), 621–629. https://doi.org/10.1175/1525-7541(2001)002<0621:EORIC>2.0.CO;2

Harter, H. L. (1984). Another look at plotting positions. *Communications in Statistics - Theory and Methods*, *13*(13), 1613–1633. https://doi.org/10.1080/03610928408828781

Jørgensen, H. K., Rosenørn, S., Madsen, H., & Mikkelsen, P. S. (1998). Quality control of rain data used for urban runoff systems. *Water Science and Technology*, *37*(11), 113–120. https://doi.org/10.1016/S0273-1223(98)00323-0

Laherrère, J., & Sornette, D. (1998). Stretched exponential distributions in nature and economy: "Fat tails" with characteristic scales. *The European Physical Journal B - Condensed Matter and Complex Systems*, *2*(4), 525–539. https://doi.org/10.1007/s100510050276

Makkonen, L. (2006). Plotting positions in extreme value analysis. *Journal of Applied Meteorology and Climatology*, *45*(2), 334–340. https://doi.org/10.1175/JAM2349.1

Menne, M. J., Durre, I., Vose, R. S., Gleason, B. E., & Houston, T. G. (2012). An overview of the global historical climatology network-daily database. *Journal of Atmospheric and Oceanic Technology*, *29*(7), 897–910. https://doi.org/10.1175/JTECH-D-11-00103.1

Restrepo-Posada, P. J., & Eagleson, P. S. (1982). Identification of independent rainstorms. *Journal of Hydrology*, *55*(1-4), 303–319. https://doi.org/10.1016/0022-1694(82)90136-6

Schroeer, K., Kirchengast, G., & Sungmin, O. (2018). Strong dependence of extreme convective precipitation intensities on gauge network density. *Geophysical Research Letters*, *45*(16), 8253–8263. https://doi.org/10.1029/2018GL077994

Schwanghart, W., & Scherler, D. (2014). Short communication: TopoToolbox 2—MATLAB-based software for topographic analysis and modeling in Earth surface sciences. *Earth Surface Dynamics*, *2*(1), 1–7. https://doi.org/10.5194/esurf-2-1-2014

Strudley, M. W., Muray, A. B., & Haff, P. K. (2006). Regolith thickness instability and the formation of tors in arid environments. *Journal of Geophysical Research - Earth Surface*, *111*(F3). https://doi.org/10.1029/2005JF000405

Upton, G. J. G., & Rahimi, A. R. (2003). On-line detection of errors in tipping-bucket raingauges. *Journal of Hydrology*, *278*(1-4), 197–212. https://doi.org/10.1016/S0022-1694(03)00142-2

Wilson, P. S., & Toumi, R. (2005). A fundamental probability distribution for heavy rainfall. *Geophysical Research Letters*, *32*,L14812. https://doi.org/10.1029/2005GL022465

Zorzetto, E., Botter, G., & Marani, M. (2016). On the emergence of rainfall extremes from ordinary events. *Geophysical Research Letters*, *43*, 8076–8082. https://doi.org/10.1002/2016GL069445